

Synthesis and Crystal Structures of Zn(II)- and Mn(II)- Diphenyldicarboxylate Complexes with N-Donor Ligand

Bon Kweon Koo

Department of Chemistry, Catholic University of Daegu, Gyeongbuk 38453, Korea.

E-mail: bkkoo@cu.ac.kr

(Received July 15, 2016; Accepted August 14, 2016)

ABSTRACT. Two new polymeric complexes, $[\text{Zn}(\text{dpa})(\text{pyz})_{0.5}]_n$ (**1**; dpa = diphenate and pyz = pyrazine) and $[\text{Mn}_3(\text{bpdc})_3(\text{py})_4]_n$ (**2**; bpdc = biphenyl-4,4'-dicarboxylate and py = pyridine) were successfully isolated by the hydro- and solvo-thermal technique, respectively. The complexes were characterized by elemental and thermal analysis, vibrational IR spectroscopy, and by single crystal x-ray structure determination. For **2**, magnetic property was also investigated. Complex **1** is a two-dimensional layer structure consisting of a paddle-wheel building unit of Zn-dpa chains bridged by pyrazine. While, complex **2** consists of linear trimeric Mn₃ cluster as building unit to form 3D network. In the complexes, dpa^{2-} (**1**) and bpdc^{2-} (**2**) ligands show a typical bis-monodendate bridging and two kinds of bridging modes: a typical bridging and chelating/bridging mode, respectively.

Key words: Crystal structure, Mn(II), Zn(II), Dicarboxylate, N-Donor

INTRODUCTION

Recently metal-organic framework (MOF) materials are attracting much interest, not only because of their intriguing structures,¹ but also due to their potential applications as functional materials.^{2–4} Dicarboxylic acid, such as diphenic acid and biphenyl-4,4'-dicarboxylic acid is a good candidate ligand for the design and construction of multidimensional metal-organic networks since the ligand has rich coordination modes^{5,6} and forms hydrogen bonding interactions through the oxygen atoms of the carboxylate group.^{7,8}

The combination of carboxylate-containing ligand and neutral pyridyl-containing ligand is also successful strategy in building supramolecular networks, using one ligand to construct basic units and another auxiliary ligand to extend the framework.^{9,10} At the same time, the utilization of mixed-ligand can give much more assembly process with metal ions through changing one of two types of organic ligands.¹¹ However, as is well known, the coordination nature of metal ions, the structural characteristic and metal affinity of organic ligands, stoichiometry of reactants, pH of the solution, and counter ions are crucial factors in the assembly process of coordination polymers. Sometimes, a small variation in any of these factors can lead to new complexes with different structural topologies.^{12,13} Therefore, it is difficult to predict either the composition or structure of the product. And so much work is required for that.

During studies aimed at constructing multi-dimensional frameworks using dicarboxylate ions,^{14,15} we have isolated

2D and 3D-coordination polymers, $[\text{Zn}(\text{dpa})(\text{pyz})_{0.5}]_n$ (**1**) and $[\text{Mn}_3(\text{bpdc})_3(\text{py})_4]_n$ (**2**) based on the mixed-ligand of dicarboxylate and N-donor ligands, respectively. In this paper, we describe the synthesis and crystal structures of the complex **1** and **2**. In addition, the thermal and magnetic property of the complexes is discussed.

EXPERIMENTAL

All chemicals are commercially available and were used as received without further purification. Elemental analyses (C, H, N) were performed on a Carlo Erba EA-1106 Elemental Analyzer. Infrared spectra were recorded in the range from 4000 to 400 cm^{-1} on a Mattson Polaris FT-IR Spectrophotometer using KBr pellets. Thermogravimetric analysis (TG) was performed on a TA Discovery TGA instrument with a heating rate of 10 $^{\circ}\text{C}\cdot\text{min}^{-1}$. The magnetization of complex **2** was measured using a Quantum Design MPMS SQUID magnetometer. All reactions were carried out in 23 ml Teflon-lined stainless-steel autoclave. The vessels were filled approximately to 40% capacity. The initial and final pH of the reaction was measured using Sentron 1001 pH meter.

Preparation of $[\text{Zn}(\text{dpa})(\text{pyz})_{0.5}]_n$ (**1**)

A mixture of $\text{Zn}(\text{OAc})_2\cdot 2\text{H}_2\text{O}$ (0.111 g, 0.5 mmol), diphenic acid (0.121 g, 0.5 mmol), pyrazine (0.040 g, 0.5 mmol), and H_2O (10 ml) in the mole ratio of 1.0:1.0:1.0:1111 was placed in a 23 ml Teflon-lined Parr acid digestion bomb

and heated for 3 d at 180 °C under autogenous pressure. After the mixture was removed from the oven and allowed to cool under ambient conditions for 3 d., large colorless needles of **1** suitable for X-ray diffraction were isolated in 53% (0.095 g) yield based on zinc. Initial pH, 4.0; final pH, 4.0. Anal. Calc. for $C_{16}H_{10}NO_4Zn$: C, 55.60; H, 2.92; N, 4.05. Found: C, 55.33; H, 3.03; N, 4.30%. IR (KBr pellet, cm^{-1}): 3100(w), 1635(s), 1592(m), 1540(m), 1471(w), 1427(m), 1396(s), 1286(w), 1160(w), 1133(w), 1078(w), 1065(w), 839(w), 757(m), 708(m), 678(m).

Preparation of $[Mn_3(bpdc)_3(py)_4]_n$ (**2**)

A mixture of $Mn(OAc)_2 \cdot 4H_2O$ (0.098 g, 0.4 mmol), 4,4'-bpdcH₂ (0.096 g, 0.4 mmol), pyridine (3.0 ml), and dimethylformamide (7.0 ml) was placed in a 23 ml Teflon-lined Parr acid digestion bomb and heated for 3 d at 160 °C under autogenous pressure. After the mixture was removed from the oven and allowed to cool under ambient conditions for 3 d, yellow crystals (block) of **2** suitable for X-ray diffraction were isolated in 40.0% (0.064 g) yield based on Mn. Anal.

Calc. for $C_{62}H_{44}N_4O_{12}Mn_3$: C, 61.96; H, 3.69; N, 4.66. Found: C, 61.85; H, 3.73; N, 4.75%. IR (KBr pellet, cm^{-1}): 2980(m), 1635(s), 1603(m), 1577(m), 1542(m), 1523(m), 1393(s), 1054(m), 1034(m), 1006(m), 768(m), 675(m).

X-ray structure determination

Single crystals of **1** and **2** were obtained by the method described in the above procedures. Structural measurement for the complexes were performed on a Bruker SMART APEX CCD diffractometer using graphite monochromatized Mo-K α radiation ($\lambda = 0.71073$ Å) at the Korea Basic Science Institute. The structures were solved by direct method and refined on F² by full-matrix least-squares procedures using the SHELXTL programs.¹⁶ All non-hydrogen atoms were refined using anisotropic thermal parameters. The hydrogen atoms were included in the structure factor calculation at idealized positions by using a riding model, but not refined. Images were created with the DIAMOND program.¹⁷ The crystallographic data for complex **1** and **2** is listed in Table 1.

Table 1. Crystal data and structure refinement for complexes **1** and **2**

Complex	1	2
Empirical formula	$C_{16}H_{10}NO_4Zn$	$C_{62}H_{44}Mn_3N_4O_{12}$
Formula weight	345.62	1201.830
T (K)	200(2)	200(2)
λ (Å)	0.71073	0.71073
Crystal system	Monoclinic	Monoclinic
Space group	C2/c	C2/c
<i>a</i> (Å)	17.801(2)	25.495(2)
<i>b</i> (Å)	21.549(2)	17.9875(17)
<i>c</i> (Å)	7.2749(6)	12.3012(11)
β (°)	92.798(2)	90.845(2)
<i>V</i> (Å ³)	2787.3(4)	5640.5(9)
<i>Z</i>	8	4
μ (mm ⁻¹)	1.779	0.728
<i>F</i> (000)	1400	2460
θ (°)	1.48 to 26.04	1.39 to 26.02
Absorption correction	Multi-scan $T_{min} = 0.7173$, $T_{max} = 0.9486$	Multi-scan $T_{min} = 0.9242$, $T_{max} = 0.9508$
Limiting indices	$-20 \leq h \leq 21$, $-26 \leq k \leq 17$, $-8 \leq l \leq 8$	$-28 \leq h \leq 31$, $-18 \leq k \leq 22$, $-15 \leq l \leq 15$
Reflections collected	8392	17485
Independent reflections	2713 [$R_{int} = 0.0266$]	5555 [$R_{int} = 0.0545$]
Observed reflections [$I \geq 2\sigma(I)$]	2349	3580
Goodness-of-fit on F^2	1.193	1.118
R_1 [$I \geq 2\sigma(I)$]	0.0352	0.0749
wR_2 [$I \geq 2\sigma(I)$]	0.0870	0.2053
R_1	0.0467	0.1172
wR_2	0.1206	0.2486
Largest peak and hole (e Å ⁻³)	0.822 and -0.760	1.280 and -0.790

RESULTS AND DISCUSSION

Complex **1** is a two-dimensional layer structure consisting of one-dimensional dpa-Zn chains bridged by pyrazine. As shown in *Fig. 1a*, two Zn(II) ions are bridged by four carboxyl groups from four different dpa²⁻ ligands, forming a paddle-wheel building unit (BU). Each Zn(II) center adopts a five-coordinate square-pyramidal ($\tau = 0.332^{(18)}$) in a ZnO₄N fashion, in which four oxygen atoms from different carboxylate groups of four dpa²⁻ comprise the pyramidal plane and one nitrogen atom from pyrazine occupies the axial position. The Zn(II) ion displaces 0.342(1) Å out of the equatorial plane (mean deviation; 0.172(3) Å). The metal-metal distance (Zn1...Zn1') in the dinuclear BU of **1** is 2.894(1) Å, that is shorter than 2.953(1) Å of the

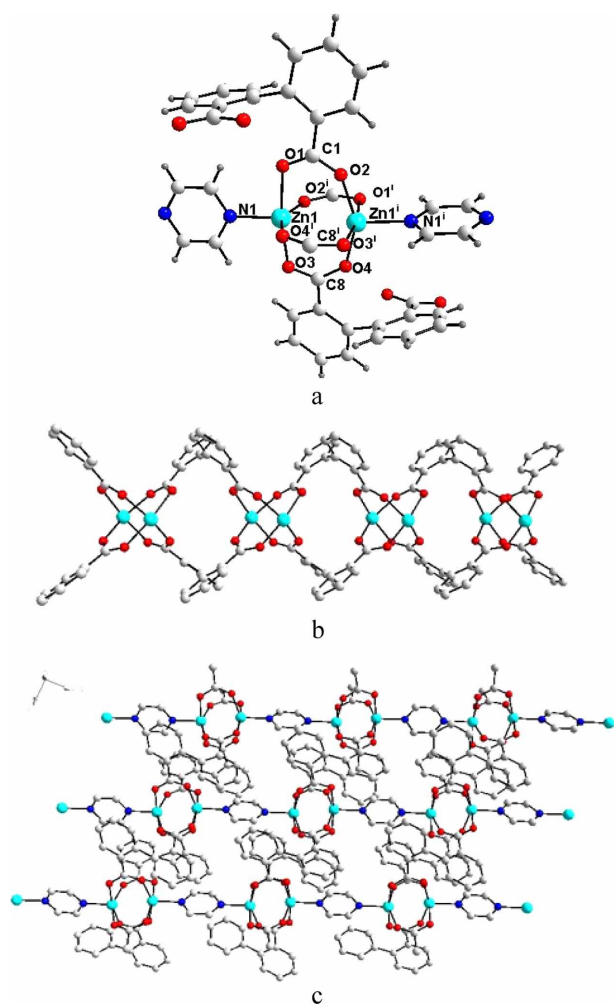
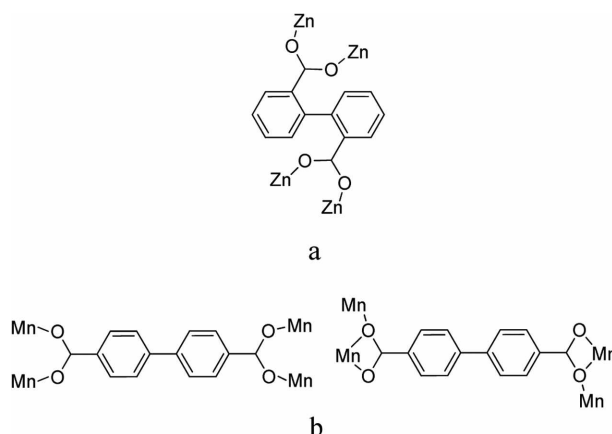


Figure 1. a Coordination environment of Zn(II) ion in complex **1**. Symmetry codes: (i) 1-x, y, 1/2-z. b Structure of 1D chain in complex **1** containing paddle-type dinuclear Zn units. All pyrazine molecules and H atoms are omitted for clarity. c 2D network of complex **1**. All H atoms are omitted for clarity.



Scheme 1. The coordination modes of ligands in **1(a)** and **2(b)**.

discrete dinuclear complex, $[\text{Zn}_2(\text{O}_2\text{CPh})_4(\text{quinoxaline})_2]$.¹⁹

The carboxyl groups in dpaH₂ are completely deprotonated (*Scheme 1a*), and just act as the gemel, forming a 1-D infinite double chain along the c-axis (*Fig. 1b*). The phenyl rings of dpa²⁻ in **1** are not co-planar, with the dihedral angle of 86.1(1)°. Two adjacent Zn-dpa²⁻ chains are joined together through the pyrazine, forming a 2-D layer structure (*Fig. 1c*). The pyrazine rings are nearly planar [mean deviation 0.004(5) Å]. The angle between two pyrazine planes in 1D chain is approximate vertical with the dihedral angle of 82.2(2)°. The two pyrazine rings belong to the adjacent chains are nearly coplanar [dihedral angle; 0.0(2)°]. Recently, the Ni(II), Cu(II), and Zn(II) complexes with the paddlewheel building unit have been reported.^{19,20} But, the complexes show the 1D chain structures constructed by metal(II)-dpa²⁻ or benzoate and 2D framework finally formed by C-H... π interactions or other spacers. It is noteworthy that the complex **1** consists of two-dimensional double chains of dpa-Zn bridged by pyrazine. The Zn-O and Zn-N distances are similar to those of paddle-wheel type Zn(II) complexes¹⁹ (*Table S1*). The C-O bond distances and O-C-O bond angles of carboxyl groups are in the range of 1.252(5)-1.264(5) Å and 124.3(4)-125.5(4)°, respectively.²¹

Complex **2** consists of linear trimeric Mn₃ clusters building block units (*Fig. 2a*, Mn1-Mn2 = 3.579(1) Å), which are linked by six carboxylate groups of the bpd²⁻ ligands to form a neutral three-dimensional network. The central Mn(II) ion is coordinated octahedrally by six carboxylate oxygen atoms, while the two Mn(II) ions in both sides are coordinated by four carboxylate oxygen atoms and two pyridine molecules in a more distorted octahedral geometry, respectively. The bond angles around the central manganese and the two manganese ions at the two ends are as followings: *trans*-L-M-L = 180(18) and *cis*-L-M-L = 85.62(14)-

94.38(14)° for Mn1, $\text{trans-L-M-L} = 160.54(17)$ – $170.64(18)$ and $\text{cis-L-M-L} = 58.25(14)$ – $105.67(15)$ ° for Mn2, respectively (Table S1).

In the complex, bpdc^{2-} ligands show two kinds of coordination mode to the metal ion (Scheme 1b): one mode is a typical bridging mode (μ_4 -bridge) and the other is the unusual coordination mode that chelates to one Mn2 atom and, at the same time, bridges the other Mn1 atom (μ_4 -chelate/bridge).¹⁹ The coordination mode of bpdc^{2-} ligand affects the extent of the distortion from the ideal octahedral arrangement. Compared to a typical bridging mode, the unusual coordination mode of carboxylate group causes a big distortion from octahedral environment around Mn2. In the typical bridging carboxylate coordination mode, Mn1–O_{bridging} distance is 2.154(3) Å (Mn1–O1, Mn1–O3), and Mn2–O_{bridging} distances are 2.092(4) (Mn2–O2) and 2.126(4) Å (Mn2–O4). In the unusual coordination mode, Mn1–O_{bridging} distance is 2.249(4) (Mn1–O5) which is a little longer than typical one, and Mn2–O_{chelating} distances are 2.268(4) (Mn2–O5) and 2.235(4) Å (Mn2–O6). In addition, the dihedral angles between two phenyl rings of bpdc^{2-} in typical and unusual coordination mode are different. The phenyl rings (C2–C7 and C2ⁱⁱⁱ–C7ⁱⁱⁱ) of bpdc^{2-} in μ_4 -bridge mode are nearly coplanar with the dihedral angle of 0.0(3)°, on the contrary to the dihedral angle 77.1(2)° between two planes, C16–C21 and C16ⁱⁱ–C21ⁱⁱ in μ_4 -chelate/bridge mode.

Each bpdc^{2-} ligand as μ_4 -bridge links two Mn–Mn units of BU to yield 2D microporous rhombic grid with cavities size of ca. 15.6×15.6 Å² (Fig. 2b). Besides, another interesting feature is the packing of the 2D grids through the remaining bpdc^{2-} ligand with μ_4 -chelate/bridge fashion that creates rhombic microporous channels (ca. $15.6 \times 15.6 \times 14.1$ Å³) in an ABAB fashion (Fig. 2c). The pyridine molecules are nearly planar with mean deviations 0.011(1) and 0.038(7) Å for N1ⁱC22ⁱ–C26ⁱ and N2ⁱC27ⁱ–C31ⁱ, respectively. The angle between two planes is 79.7(3)°. Mn–N (average) bond distance is 2.262(5) Å which is typical in Mn complexes.²² The C–O bond distances and O–C–O bond angles of carboxyl groups are in the range of 1.254(6)–1.272(7) Å and 120.4(5)–125.7(5)°, respectively as shown in complex 1.

The IR spectra show a typical antisymmetric and symmetric stretching bands of carboxylate groups at 1540 and 1396 cm^{−1} for 1 and at 1542, 1523 and 1393 cm^{−1} for 2, respectively.^{23,24} The separation (Δ) between $\nu_{\text{asym}}(\text{CO}_2)$ and $\nu_{\text{sym}}(\text{CO}_2)$ is 144 cm^{−1} for 1 and 149 and 130 cm^{−1} for 2, respectively. This value is similar to the Δ value calculated ($\Delta = 1818.1 \delta_r + 16.47 (\theta_{\text{OCO}} - 120) + 66.8$, where δ_r is difference between the two CO bond lengths (Å) and θ_{OCO} is the

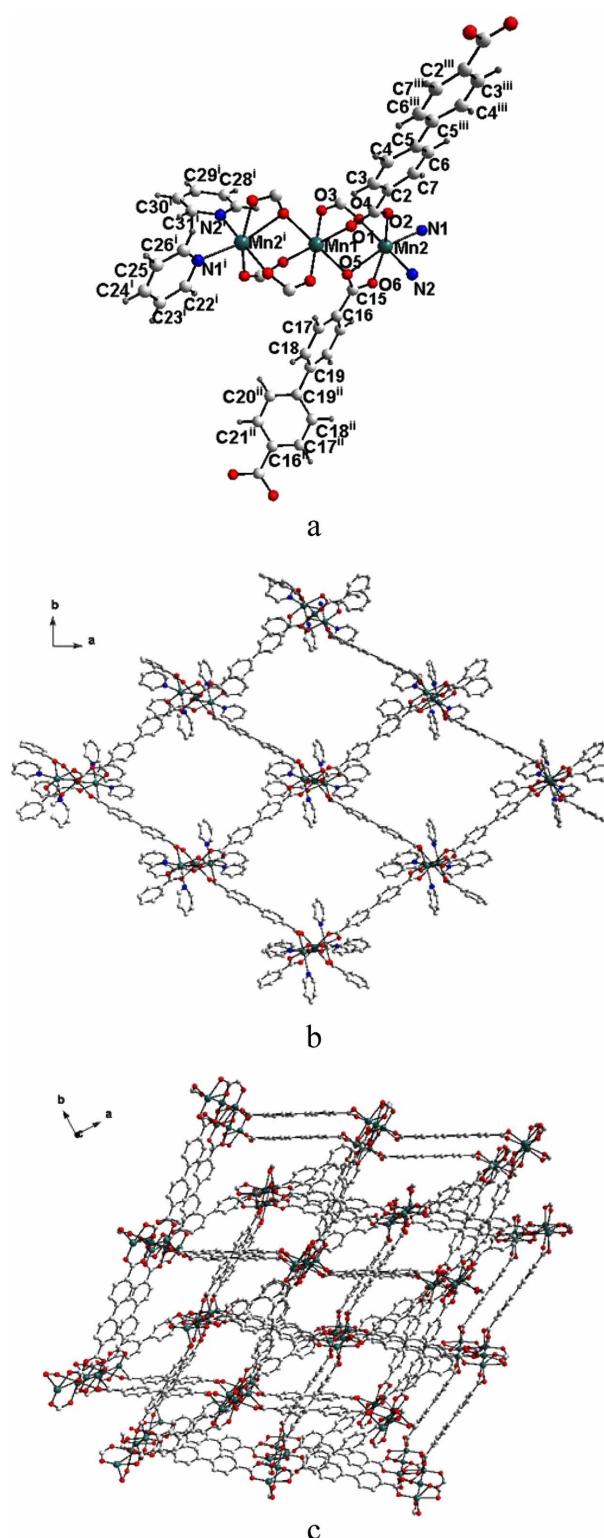


Figure 2. a Coordination environment of Mn(II) ion in complex 2. The six carboxylic groups link the three Mn atoms to the trinuclear BU. Symmetry code: (i) $1/2-x, 1/2-y, 1-z$; (ii) $-x, y, 1/2-z$; (iii) $1-x, y, 1-z$. b A 2D layer. c View showing the stacking pattern of the 2D network of square grids. Pyridine molecules are omitted for clarity.

OCO angle ($^{\circ}$)²⁵) from the structural data of the complex **1** and **2**: 154 cm^{-1} for **1** and 144 and 132 cm^{-1} for **2**, respectively. The value in Δ is attributed to the bridging (for **1**) or bridging/chelating (for **2**) coordination mode of carboxylate groups to the metal,²⁶ respectively (Scheme 1). The peaks at 1603-1635 and 1577-1592 cm^{-1} are attributable to the $\nu(\text{C}=\text{N})$ or $\nu(\text{C}=\text{C})$ of aromatic group.²⁷

TG analysis of compound **1** and **2** was performed to observe their thermal behaviors. As shown in Fig. 3, both complexes show two steps of weight losses. Complex **1** is stable up to 165 $^{\circ}\text{C}$ and then it displays two steps weight loss to 465 $^{\circ}\text{C}$ (exp. 70.2%), corresponding to the loss of organic ligands (calc. 81.1%). They are overlapped to each other and the ligands collapse slowly beyond this temperature to the 700 $^{\circ}\text{C}$. While, the first weight loss for **2** is 23.84% at 30-396 $^{\circ}\text{C}$, assigned to the loss of pyridine molecules (calc. 26.35%). The second weight loss is going on and continues up to 700 $^{\circ}\text{C}$, corresponding to the further decomposing of the compound. The total weight loss of 59.73% is much less than the calculated value of 82.29% if the final product is assumed to be MnO , which indicate that the decomposing process is not complete due to the use of

nitrogen protection.

The temperature dependence of the magnetic susceptibility for **2** was investigated in the temperature range from 5 to 300 K under an applied magnetic field of 1000 Oe. The variation of $\chi_{\text{m}}T$ and χ_{m} with T is shown in Fig. 4. At 300 K, the $\chi_{\text{m}}T$ is 1.28 $\text{emu mol}^{-1} \text{K}$. As temperature is lowered, the $\chi_{\text{m}}T$ value decreases continuously to a value of 0.312 $\text{emu mol}^{-1} \text{K}$ at 5 K. Such a behavior of $\chi_{\text{m}}T$ curve indicates a mainly antiferromagnetic interaction in **2**.²⁸ The variation of the χ_{m} with temperature follows the Curie-Weiss equation because of the linear relationship between χ_{m}^{-1} and T . The Curie constant and Weiss temperature are found to be 1.43 $\text{emu mol}^{-1} \text{K}$ and -18.35 K. The negative Weiss temperature further indicates the antiferromagnetic interactions between Mn(II) ions.^{22,29}

CONCLUSION

Two new polymeric complexes, $[\text{Zn}(\text{dpa})(\text{pyz})_{0.5}]_n$ (**1**) and $[\text{Mn}_3(\text{bpdc})_3(\text{py})_4]_n$ (**2**) were successfully isolated by the hydro- and solvo-thermal technique, respectively. Complex **1** is a two-dimensional layer structure consisting of a paddle-wheel building unit of Zn-dpa chains bridged by pyrazine. While, complex **2** consists of linear trimeric Mn_3 cluster as BU to form 3D network. In the complex, the bpdc^{2-} ligands show two kinds of bridging modes: a typical bridging and chelating/bridging mode. It shows that the coordination modes of ligand to the metal play an important role in the structural diversity of metal complex. The results also suggest an example of 2D and 3D network metal(II) complexes with diphenate/pyrazine and biphenyl-4,4'-dicarboxylate/pyridine system, respectively. In addition, magnetic property for complex **2** indicates the antiferromagnetic interactions between Mn(II) ions

Acknowledgments. This research was supported by the Research Grants of Catholic University of Daegu in 2013. The author also acknowledges the Korea Basic Science Institute for providing the crystal structure results.

Supplementary Materials. Crystallographic data for the structures reported here have been deposited with CCDC (Deposition No. CCDC-1023044 (**1**) and CCDC-1415030 (**2**)). These data can be obtained free of charge via <http://www.ccdc.cam.ac.uk/conts/retrieving.html> or from CCDC, 12 Union Road, Cambridge CB2 1EZ, UK, E-mail: deposit@ccdc.cam.ac.uk. Selected bond lengths and angles for the complexes **1** and **2** (Table S1) are available in the online version of this article.

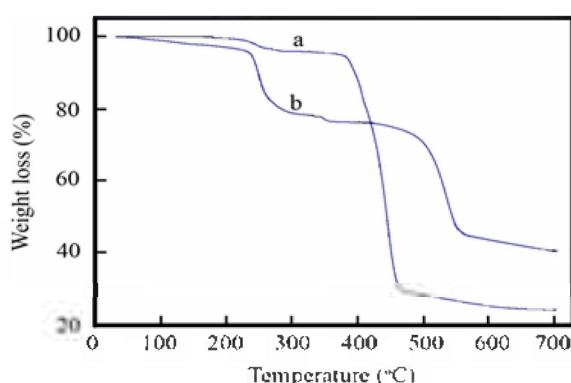


Figure 3. TGA curves of complex **1**(a) and **2**(b).

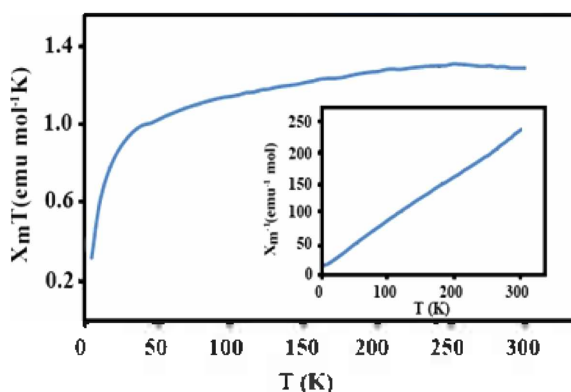


Figure 4. The magnetic property of complex **2**.

REFERENCES

1. Lin, Z.-J.; Lu, J.; Hong, M.; Cao, R. *Chem. Soc. Rev.* **2014**, *43*, 5867.
2. Aguado, S.; Quiros, J.; Canivet, J.; Farrusseng, D.; Boltes, K.; Rosal, R. *Chemosphere* **2014**, *113*, 188.
3. Hermann, D.; Emerich, H.; Lepski, R.; Schaniel, D.; Ruschewitz, U. *Inorg. Chem.* **2013**, *52*, 2744.
4. Dimos, K.; Stathi, P.; Karakassides, M. A.; Deligiannakis, Y. *Microporous Mesoporous Mat.* **2009**, *126*, 65.
5. Su, Z.; Fan, J.; Chen, M.; Okamura, T.-A.; Sun, W.-Y. *Cryst. Growth Des.* **2011**, *11*, 1159.
6. Xu, G.-H.; Ma, Y.; Wang, K.; Wang, X.; Gao, E.-Q. *J. Mol. Struct.* **2013**, *1040*, 25.
7. Soleimannejad, J.; Nazarnia, E.; Helen, S.-E. *J. Mol. Struct.* **2014**, *1076*, 620.
8. Montney, M. R.; Supkowski, R. M.; LaDuca, R. L. *CrystEngComm.* **2008**, *10*, 111.
9. Niu, D.; Yang, J.; Guo, J.; Kan, W.-Q.; Song, S.-Y.; Du, P.; Ma, J.-F. *Cryst. Growth Des.* **2012**, *12*, 2397.
10. Cao, X.; Mu, B.; Huang, R. *CrystEngComm.* **2014**, *16*, 5093.
11. Yang, J.-X.; Zhai, J.-Q.; Zhang, X.; Qin, Y.-Y.; Yao, Y.-G. *Dalton Trans.* **2016**, *45*, 711.
12. Wang, R.-H.; Gong, Y.-Q.; Han, L.; Yuan, D.-Q.; Lou, B.-Y.; Wu, B.-L.; Hong, M.-C. *J. Mol. Struct.* **2006**, *784*, 1.
13. Köberl, M.; Cokoja, M.; Hermann, W. A.; Kühn, F. E. *Dalton Trans.* **2011**, *40*, 6834.
14. Koo, B. K. *Bull. Korean Chem. Soc.* **2012**, *33*, 2299.
15. Koo, B. K.; Kim, J.; Lee, U. *Inorg. Chim. Acta* **2010**, *363*, 1760.
16. Sheldrick, G. M., SHELXTL. Version 6. Bruker AXS Inc. Madison, Wisconsin, USA, 2001.
17. Brandenburg, K. DIAMOND. Version 2.1. Crystal Impact GbR, Bonn, Germany. 1998.
18. Gaurav, B.; Inke, J.; Christian, N. *Inorg Chem* **2006**, *45*, 6508.
19. Kwak, H.; Lee, S. H.; Kim, S. H.; Lee, Y. M.; Park, B. K.; Lee, E. Y.; Lee, Y. J.; Kim, C.; Kim, S. J.; Kim, Y. *Polyhedron* **2008**, *27*, 3484.
20. Shi, Q.; Sun, Y.; Sheng, L.; Ma, K.; Cai, X.; Liu, D. *Inorg. Chim. Acta* **2009**, *362*, 4167.
21. Qi, X.-L. *Acta Cryst.* **2009**, *39*, 3845.
22. Li, N.; Chen, L.; Lian, F.; Jiang, F.; Hong, M. *Inorg. Chim. Acta* **2010**, *363*, 3291.
23. Wang, Y.-L.; Jiang, Y.-L.; Xiahou, Z.-J.; Fu, J.-H.; Liu, Q.-Y. *Dalton Trans.* **2012**, *41*, 11428.
24. Zhou, H.; Yu, M.; Liu, G.-X. *Inorg. Chim. Acta* **2016**, *439*, 130.
25. Vargová, Z.; Zeleňák, V.; Císařová, I.; Györyová, K. *Thermochim. Acta* **2004**, *423*, 149.
26. Zelén, V.; Vargová, Z.; Györyová, K. *Spectrochim. Acta Part A* **2007**, *66*, 262.
27. Kim, J.; Lee, U.; Koo, B. K. *Bull. Korean Chem. Soc.* **2010**, *31*, 1743.
28. Liu, B.; Zou, R. Q.; Zhong, R. Q.; Han, S.; Shioyama, H.; Yamada, T.; Maruta, G.; Taketa, S.; Xu, Q. *Micropor. Mesopor. Mat.* **2008**, *111*, 470.
29. Kongshaug, K. O.; Fjellvag, H. *Solid State Sci.* **2002**, *4*, 443.